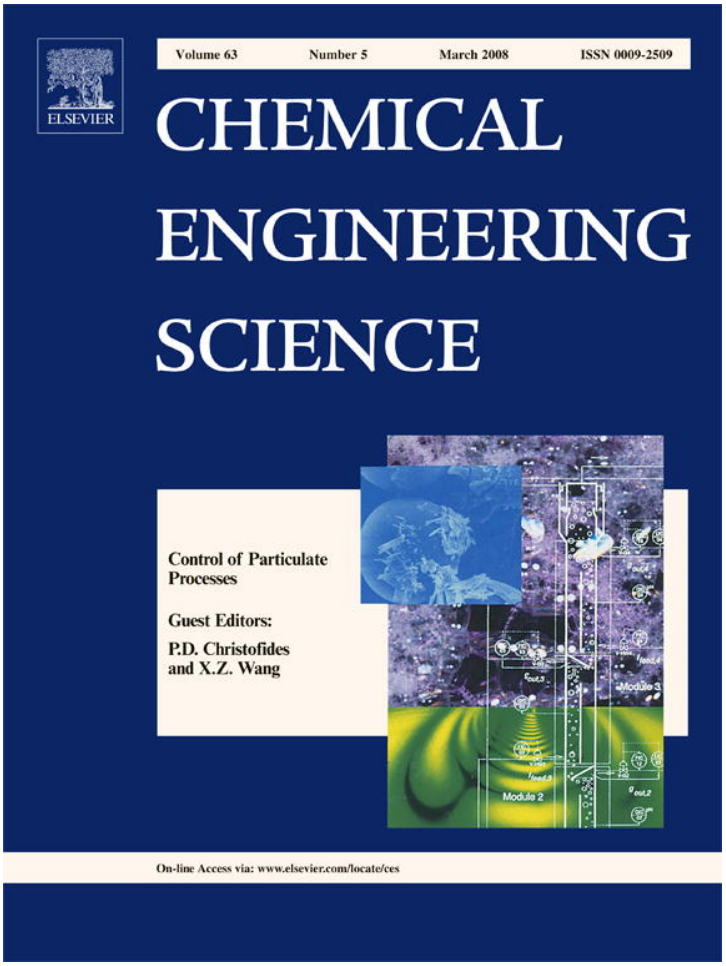

ELSEVIER

Chemical Engineering Science 63 (2008) 1156–1172

Chemical Engineering Science

www.elsevier.com/locate/ces

Model-based control of particulate processes

Panagiotis D. Christofides[a,b,*], Nael El-Farra[c], Mingheng Li[d], Prashant Mhaskar[e]

[a]*Department of Chemical and Biomolecular Engineering, University of California, Los Angeles, CA 90095, USA*
[b]*Department of Electrical Engineering, University of California, Los Angeles, CA 90095, USA*
[c]*Department of Chemical Engineering and Materials Science, University of California, Davis, CA 95616, USA*
[d]*Department of Chemical and Materials Engineering, California State Polytechnic University, Pomona, CA 91768, USA*
[e]*Department of Chemical Engineering, McMaster University, Ont., Canada L8S 4L7*

Available online 20 July 2007

Abstract

In this work, we present an overview of recently developed methods for model-based control of particulate processes. We primarily discuss methods developed in the context of our previous research work and use examples of crystallization, aerosol and thermal spray processes to motivate the development of these methods and illustrate their application. Specifically, we initially discuss control methods for particulate processes which utilize suitable approximations of population balance models to design nonlinear, robust and predictive control systems and demonstrate their application to crystallization and aerosol processes. Finally, we discuss the issues of control problem formulation and controller design for high-velocity oxygen-fuel (HVOF) thermal spray processes and close with few thoughts on unresolved research challenges on control of particulate processes.

Keywords: Particulate processes; Order reduction; Model-based feedback control; Crystallization; Aerosol processes; Thermal spray processes

1. Introduction

Particulate processes (also known as dispersed-phase processes) are characterized by the co-presence of and strong interaction between a continuous (gas or liquid) phase and a particulate (dispersed) phase and are essential in making many high-value industrial products. Particulate processes play a prominent role in a number of process industries since about 60% of the products in the chemical industry are manufactured as particulates with an additional 20% using powders as ingredients. Representative examples of industrial particulate processes include the crystallization of proteins for pharmaceutical applications, the emulsion polymerization for the production of latex, the fluidized bed production of solar-grade silicon particles through thermal decomposition of silane gas, the aerosol synthesis of titania powder used in the production of white pigments, and the thermal spray processing of nanostructured thermal barrier and wear resistant coatings. The industrial importance of particulate processes and the realization that the physicochemical and mechanical properties of materials made with particulates depend heavily on the characteristics of the underlying particle-size distribution (PSD) have motivated significant research attention over the last 10 years on model-based control of particulate processes. These efforts have also been complemented by recent and on-going developments in measurement technology which allow the accurate and fast on-line measurement of key process variables including important characteristics of PSDs (e.g., Larsen et al., 2006; Rawlings et al., 1992, 1993). The recent efforts on model-based control of particulate processes have also been motivated by significant advances in the modeling of particulate processes. Specifically, population balances have provided a natural framework for the mathematical modeling of PSDs in broad classes of particulate processes (see, for example, the tutorial article (Hulburt and Katz, 1964) and the review article (Ramkrishna, 1985)), and have been successfully used to describe PSDs in emulsion polymerization reactors (e.g., Dimitratos et al., 1994; Doyle et al., 2002), crystallizers (e.g., Braatz and Hasebe, 2002; Rawlings et al., 1993), aerosol reactors (e.g., Friendlander,

* Corresponding author. Department of Chemical and Biomolecular Engineering, University of California, Los Angeles, CA 90095, USA. Tel.: +1 310 794 1015; fax: +1 310 206 4107.
E-mail address: pdc@seas.ucla.edu (P.D. Christofides).

0009-2509/$ - see front matter © 2007 Elsevier Ltd. All rights reserved.
doi:10.1016/j.ces.2007.07.017

2000) and cell cultures (e.g., Daoutidis and Henson, 2001). To illustrate the structure of the mathematical models that arise in the population balance modeling of particulate processes, we focus on three representative examples: a continuous crystallizer, a batch crystallizer and an aerosol reactor.

1.1. Continuous crystallization

Crystallization is a particulate process which is widely used in industry for the production of many products including fertilizers, proteins and pesticides. Specifically, we consider a typical continuous crystallization process (Jerauld et al., 1983; Lei et al., 1971). Under the assumptions of isothermal operation, constant volume, mixed suspension, nucleation of crystals of infinitesimal size and mixed product removal, a dynamic model for the crystallizer can be derived from a population balance for the particle phase and a mass balance for the solute concentration and has the following mathematical form (Jerauld et al., 1983; Lei et al., 1971):

$$\frac{\partial n(r,t)}{\partial t} = -\frac{\partial (R(t)n(r,t))}{\partial r} - \frac{n(r,t)}{\tau} + \delta(r-0)Q(t),$$

$$\frac{\mathrm{d}c(t)}{\mathrm{d}t} = \frac{(c_0-\rho)}{\varepsilon(t)\tau} + \frac{(\rho-c(t))}{\tau} + \frac{(\rho-c(t))}{\varepsilon(t)}\frac{\mathrm{d}\varepsilon(t)}{\mathrm{d}t}, \qquad (1.1)$$

where $n(r,t)$ is the number of crystals of radius $r \in [0,\infty)$ at time t per unit volume of suspension, τ is the residence time, ρ is the density of the liquid phase, $c(t)$ is the solute concentration in the crystallizer, c_0 is the solute concentration in the feed and

$$\varepsilon(t) = 1 - \int_0^\infty n(r,t)\frac{4}{3}\pi r^3 \,\mathrm{d}r$$

is the volume of liquid per unit volume of suspension. $R(t)$ is the crystal growth rate, $\delta(r-0)$ is the standard Dirac function and $Q(t)$ is the crystal nucleation rate. The term $\delta(r-0)Q(t)$ accounts for the production of crystals of infinitesimal (zero) size via nucleation. An example of expressions of $R(t)$ and $Q(t)$ is the following:

$$R(t) = k_1(c(t)-c_s), \quad Q(t) = \varepsilon(t)k_2\,\mathrm{e}^{-k_3/((c(t)/c_s)-1)^2}, \quad (1.2)$$

where k_1, k_2 and k_3 are constants and c_s is the concentration of solute at saturation. For a variety of operating conditions (see Chiu and Christofides, 1999 for model parameters and detailed studies), the continuous crystallizer model of Eq. (1.1) exhibits highly oscillatory behavior (the main reason for this behavior is that the nucleation rate is much more sensitive to supersaturation relative to the growth rate—i.e., compare the dependence of $R(t)$ and $Q(t)$ on the values of $c(t)$ and c_s) which suggests the use of feedback control to ensure stable operation and attain a crystal size distribution with desired characteristics. To achieve this control objective the inlet solute concentration can be used as the manipulated input and the crystal concentration as the controlled and measured output.

1.2. Batch protein crystallization

Batch crystallization plays an important role in pharmaceutical industry. We consider a batch crystallizer which is used to produce tetragonal HEW (hen–egg–white) lysozyme crystals from a supersaturated solution (Shi et al., 2005). Applying population, mass and energy balances to the process, the following mathematical model is obtained:

$$\frac{\partial n(r,t)}{\partial t} + G(t)\frac{\partial n(r,t)}{\partial r} = 0, \quad n(0,t) = \frac{B(t)}{G(t)},$$

$$\frac{\mathrm{d}C(t)}{\mathrm{d}t} = -24\rho k_v G(t)\mu_2(t),$$

$$\frac{\mathrm{d}T(t)}{\mathrm{d}t} = -\frac{UA}{MC_p}(T(t)-T_j(t)), \qquad (1.3)$$

where $n(r,t)$ is the crystal size distribution, $B(t)$ is the nucleation rate, $G(t)$ is the growth rate, $C(t)$ is the solute concentration, $T(t)$ is the crystallizer temperature, $T_j(t)$ is the jacket temperature, ρ is the density of crystals, k_v is the volumetric shape factor, U is the overall heat-transfer coefficient, A is the total heat-transfer surface area, M is the mass of solvent in the crystallizer, C_p is the heat capacity of the solution and $\mu_2(t) = \int_0^\infty r^2 n(r,t)\,\mathrm{d}r$ is the second moment of the crystal size distribution. The nucleation rate, $B(t)$, and the growth rate, $G(t)$, are given by (Shi et al., 2005):

$$B(t) = k_a C(t)\exp\left(-\frac{k_b}{\sigma^2(t)}\right), \quad G(t) = k_g\sigma^g(t), \qquad (1.4)$$

where $\sigma(t)$, the supersaturation, is a dimensionless variable and defined as $\sigma(t) = \ln(C(t)/C_s(T(t)))$, $C(t)$ is the solute concentration, g is the exponent relating growth rate to the supersaturation and $C_s(T)$ is the saturation concentration of the solute which is a nonlinear function of the temperature of the form

$$C_s(T) = 1.0036\times 10^{-3}T^3 + 1.4059\times 10^{-2}T^2 - 0.12835T + 3.4613. \qquad (1.5)$$

The existing experimental results (Vekilov and Rosenberger, 1996) show that the growth condition of tetragonal HEW lysozyme crystal is significantly affected by the supersaturation. Low supersaturation will lead to the cessation of the crystal growth. On the other hand, rather than forming tetragonal crystals, large amount of needle like crystals will form when the supersaturation is too high. Therefore, a proper range of supersaturation is necessary to guarantee the product's quality. The jacket temperature, T_j, is manipulated to achieve the desired crystal shape and size distribution.

1.3. Aerosol flow reactor

Aerosol processes are increasingly being used for the large-scale production of nano- and micron-sized particles. We consider a typical aerosol flow reactor with simultaneous chemical reaction, nucleation, condensation, coagulation and

convective transport. A general mathematical model which describes the spatio-temporal evolution of the PSD in such aerosol processes can be obtained from a population balance and consists of the following nonlinear partial integro-differential equation (Kalani and Christofides, 1999, 2000):

$$\frac{\partial n(v,z,t)}{\partial t} + v_z \frac{\partial n(v,z,t)}{\partial z} + \frac{\partial (G(\bar{x},v,z)n(v,z,t))}{\partial v} - I(v^*)\delta(v-v^*) = \frac{1}{2}\int_0^v \beta(v-\bar{v},\bar{v},\bar{x})n(v-\bar{v},t)n(\bar{v},z,t)\,\mathrm{d}\bar{v} - n(v,z,t)\int_0^\infty \beta(v,\bar{v},\bar{x})n(\bar{v},z,t)\,\mathrm{d}\bar{v}, \quad (1.6)$$

where $n(v,z,t)$ denotes the PSD function, v is the particle volume, t is the time, $z \in [0,L]$ is the spatial coordinate, L is the length scale of the process, v^* is the size of the nucleated aerosol particles, v_z is the velocity of the fluid, $\bar{x}$ is the vector of the state variables of the continuous phase, $G(\cdot,\cdot,\cdot)$, $I(\cdot)$, $\beta(\cdot,\cdot,\cdot)$ are nonlinear scalar functions which represent the growth, nucleation and coagulation rates and $\delta(\cdot)$ is the standard Dirac function. The model of Eq. (1.6) is coupled with a mathematical model which describes the spatio-temporal evolution of the concentrations of species and temperature of the gas phase ($\bar{x}$) that can be obtained from mass and energy balances. The control problem is to regulate process variables like inlet flow rates and wall temperature to produce aerosol products with desired size distribution characteristics.

The mathematical models of Eqs. (1.1), (1.3), (1.6) demonstrate that particulate process models are nonlinear and distributed parameters in nature. These properties have motivated extensive research on the development of efficient numerical methods for the accurate computation of their solution (see, for example, Daoutidis and Henson, 2001; Friendlander, 2000; Gelbard and Seinfeld, 1978; Lee and Matsoukas, 2000; Lin et al., 2002; Ramkrishna, 1985; Smith and Matsoukas, 1998). However, in spite of the rich literature on population balance modeling, numerical solution and dynamical analysis of particulate processes, up to about 10 years ago, research on model-based control of particulate processes had been very limited. Specifically, early research efforts had mainly focused on the understanding of fundamental control-theoretic properties (controllability and observability) of population balance models (Semino and Ray, 1995a) and the application of conventional control schemes (such as proportional-integral and proportional-integral-derivative control, self-tuning control) to crystallizers and emulsion polymerization processes (see, for example, Dimitratos et al., 1994; Rohani and Bourne, 1990; Semino and Ray, 1995b and the references therein). The main difficulty in synthesizing nonlinear model-based feedback controllers for particulate processes is the distributed parameter nature of the population balance models which does not allow their direct use for the synthesis of low-order (and therefore, practically implementable) model-based feedback controllers. Furthermore, a direct application of the aforementioned solution methods to particulate process models lead to finite dimensional approximations of the population balance models (i.e., nonlinear ordinary differential equation (ODE) systems in time) which are of very high order, and thus inappropriate for the synthesis of model-based feedback controllers that can be implemented in real-time. This limitation had been the bottleneck for model-based synthesis and real-time implementation of feedback controllers on particulate processes.

2. Model-based control of particulate processes

2.1. Overview

Motivated by the lack of population balance-based control methods for particulate processes and the need to achieve tight size distribution control in many particulate processes, we developed, over the last 10 years, a general framework for the synthesis of nonlinear, robust and predictive controllers for particulate processes based on population balance models (Chiu and Christofides, 1999, 2000; Christofides, 2002; Christofides and Chiu, 1997; El-Farra et al., 2001; Kalani and Christofides, 1999, 2002; Shi et al., 2005, 2006). Specifically, within the developed framework, nonlinear low-order approximations of the particulate process models are initially derived using order reduction techniques and are used for controller synthesis. Subsequently, the infinite-dimensional closed-loop system stability, performance and robustness properties were precisely characterized in terms of the accuracy of the approximation of the low-order models. Furthermore, controller designs were proposed that deal directly with the key practical issues of uncertainty in model parameters, unmodeled actuator/sensor dynamics and constraints in the capacity of control actuators and the magnitude of the process state variables. It is also important to note that owing to the low-dimensional structure of the controllers, the computation of the control action involves the solution of a small set of ODEs, and thus the developed controllers can be readily implemented in real-time with reasonable computing power, thereby resolving the main issue on model-based control of particulate processes. In addition to theoretical developments, we also successfully demonstrated the application of the proposed methods to size distribution control in continuous and batch crystallization, aerosol and thermal spray processes, and documented their effectiveness and advantages with respect to conventional control methods. Fig. 1 summarizes these efforts. The reader may refer to Braatz and Hasebe (2002), Daoutidis and Henson (2001), Doyle et al. (2002) for recent reviews of results on simulation and control of particulate processes.

2.2. Particulate process model

To present the main elements of our approach to model-based control of particulate processes, we focus on a general class of spatially homogeneous particulate processes with simultaneous particle growth, nucleation, agglomeration and breakage. Examples of such processes have been introduced in the previous section. Assuming that particle size is the only internal particle coordinate and applying a dynamic material

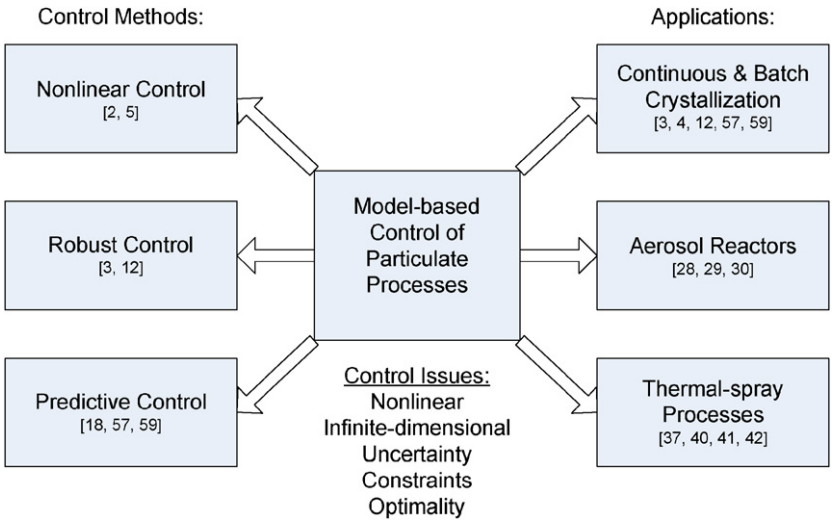

Fig. 1. Summary of our research on model-based control of particulate processes.

balance on the number of particles of size r to $r + \mathrm{d}r$ (population balance), we obtain the following general nonlinear partial integro-differential equation which describes the rate of change of the PSD, $n(r, t)$:

$$\frac{\partial n}{\partial t} = -\frac{\partial (G(x, r)n)}{\partial r} + w(n, x, r), \tag{2.7}$$

where $n(r, t)$ is the particle number size distribution, $r \in [0, r_{\max}]$ is the particle size, $r_{\max}$ is the maximum particle size (which may be infinity), t is the time and $x \in \mathbb{R}^n$ is the vector of state variables which describe properties of the continuous phase (for example solute concentration, temperature and pH in a crystallizer); see Eq. (2.8) for the system that describes the dynamics of x. $G(x, r)$ and $w(n, x, r)$ are nonlinear scalar functions whose physical meaning can be explained as follows: $G(x, r)$ accounts for particle growth through condensation and is usually referred to as growth rate. It usually depends on the concentrations of the various species present in the continuous phase, the temperature of the process and the particle size. On the other hand, $w(n, x, r)$ represents the net rate of introduction of new particles into the system. It includes all the means by which particles appear or disappear within the system including particle agglomeration (merging of two particles into one), breakage (division of one particle to two) as well as nucleation of particles of size $r \geqslant 0$ and particle feed and removal. The rate of change of the continuous-phase variables x can be derived by a direct application of mass and energy balances to the continuous phase and is given by a nonlinear integro-differential equation system of the general form:

$$\dot{x} = f(x) + g(x)u(t) + A \int_0^{r_{\max}} a(n, r, x)\, \mathrm{d}r, \tag{2.8}$$

where $f(x)$ and $a(n, r, x)$ are nonlinear vector functions, $g(x)$ is a nonlinear matrix function, A is a constant matrix and $u(t) = [u_1\ u_2\ \cdots\ u_m] \in \mathbb{R}^m$ is the vector of manipulated inputs. The term $A \int_0^{r_{\max}} a(n, r, x)\, \mathrm{d}r$ accounts for mass and heat transfer from the continuous phase to all the particles in the population.

2.3. Model reduction of particulate process models

While the population balance models are infinite-dimensional systems, the dominant dynamic behavior of many particulate process models has been shown to be low-dimensional. Manifestations of this fundamental property include the occurrence of oscillatory behavior in continuous crystallizers (Jerauld et al., 1983) and the ability to capture the long-term behavior of aerosol systems with self-similar solutions (Friendlander, 2000). Motivated by this, we introduced (Chiu and Christofides, 1999) a general methodology for deriving low-order ODE systems that accurately reproduce the dominant dynamics of the nonlinear integro-differential equation system of Eqs. (2.7) and (2.8). The proposed model reduction methodology exploits the low-dimensional behavior of the dominant dynamics of the system of Eqs. (2.7) and (2.8) and is based on a combination of the method of weighted residuals with the concept of approximate inertial manifold.

Specifically, the proposed approach initially employs the method of weighted residuals (see Ramkrishna, 1985 for a comprehensive review of results on the use of this method for solving population balance equations) to construct a nonlinear, possibly high-order, ODE system that accurately reproduces the solutions and dynamics of the distributed parameter system of Eqs. (2.7) and (2.8). Specifically, we first consider an orthogonal set of basis functions $\phi_k(r)$, where $r \in [0, r_{\max})$, $k = 1, \ldots, \infty$, and expand the PSD function $n(r, t)$ in an infinite series in terms of $\phi_k(r)$ as follows:

$$n(r, t) = \sum_{k=1}^{\infty} a_k(t)\phi_k(r), \tag{2.9}$$

where $a_k(t)$ are time-varying coefficients that characterize the system, i.e., the system state. In order to characterize the system with a finite set of ODEs, we obtain a set of N equations substituting Eq. (2.9) into Eqs. (2.7) and (2.8), multiplying the population balance with N different weighting functions $\psi_v(r)$

(that is, $v = 1, \ldots, N$), and integrating over the entire particle size spectrum. In order to obtain a finite-dimensional model, the series of expansion of $n(r, t)$ is truncated up to order N. The infinite-dimensional system of Eq. (2.7) reduces to the following finite set of ODEs:

$$\int_0^{r_{\max}} \psi_v(r) \sum_{k=1}^{N} \phi_k(r) \frac{\partial a_{kN}(t)}{\partial t} \, \mathrm{d}r$$

$$= -\sum_{k=1}^{N} a_{kN}(t) \int_0^{r_{\max}} \psi_v(r) \frac{\partial (G(x_N, r)\phi_k(r))}{\partial r} \, \mathrm{d}r$$

$$+ \int_0^{r_{\max}} \psi_v(r) w \left(\sum_{k=1}^{N} a_{kN}(t)\phi_k(r), x_N, r \right) \mathrm{d}r,$$

$$v = 1, \ldots, N,$$

$$\dot{x}_N = f(x_N) + g(x_N)u(t)$$

$$+ A \int_0^{r_{\max}} a \left(\sum_{k=1}^{N} a_{kN}(t)\phi_k(r), r, x_N \right) \mathrm{d}r, \qquad (2.10)$$

where x_N and a_{kN} are the approximations of x and a_k obtained by an Nth order truncation. From Eq. (2.10), it is clear that the form of the ODEs that describe the rate of change of $a_{kN}(t)$ depends on the choice of the basis and weighting functions, as well as on N. The system of Eq. (2.10) was obtained from a direct application of the method of weighted residuals (with arbitrary basis functions) to the system of Eqs. (2.7) and (2.8), and thus may be of very high order in order to provide an accurate description of the dominant dynamics of the particulate process model. High-dimensionality of the system of Eq. (2.10) leads to complex controller design and high-order controllers, which cannot be readily implemented in practice. To circumvent these problems, we exploited in Chiu and Christofides (1999) the low-dimensional behavior of the dominant dynamics of particulate processes and proposed an approach based on the concept of inertial manifold to derive low-order ODE systems that accurately describe the dominant dynamics of the system of Eq. (2.10). This order reduction technique initially employs singular perturbation techniques to construct nonlinear approximations of the modes neglected in the derivation of the finite-dimensional model of Eq. (2.10) (i.e., modes of order $N + 1$ and higher) in terms of the first N modes. Subsequently, these expressions for the modes of order $N + 1$ and higher (truncated up to appropriate order) are used in the model of Eq. (2.10) (instead of setting them to zero) and allow significantly improving the accuracy of the model of Eq. (2.10) without increasing its dimension; details on this procedure can be found in Chiu and Christofides (1999).

Referring to the method of weighted residuals, it is important to note that the basis and weighting functions determine the type of weighted residual method being used. In particular, the method of weighted residuals reduces to the method of moments when the basis functions are chosen to be Laguerre polynomials and the weighting functions are chosen as $\psi_v = r^v$. The moments of the PSD are defined as

$$\mu_v = \int_0^{\infty} r^v n(r, t) \, \mathrm{d}r, \quad v = 0, \ldots, \infty, \qquad (2.11)$$

and the moment equations can be directly generated from the population balance model by multiplying it by r^v, $v = 0, \ldots, \infty$ and integrating from 0 to ∞. The procedure of forming moments of the population balance equation very often leads to terms that may not reduce to moments, terms that include fractional moments, or to an unclosed set of moment equations. To overcome this problem, the PSD is expanded in terms of Laguerre polynomials defined in $L_2[0, \infty)$ and the series solution using a finite number of terms is used to close the set of moment equations (this procedure can be used for models of crystallizers with fines trap; see, for example, Chiu and Christofides, 2000).

2.4. Model-based control using low-order models

2.4.1. Nonlinear control

We constructed low-order models using the technique described in the previous section to synthesize nonlinear finite-dimensional state and output feedback controllers that guarantee stability and enforce output tracking in the closed-loop finite-dimensional system. We also established that the same controller exponentially stabilizes the closed-loop particulate process model. The output feedback controller is constructed through a standard combination of the state feedback controller with a state observer. The state feedback controller is synthesized via geometric control methods and the state observer is an extended Luenberger-type observer (see Chiu and Christofides, 1999 for detailed controller synthesis formulas). We performed several simulations in the context of the continuous crystallizer process model presented before to evaluate the performance and robustness properties of the nonlinear controllers designed based on the reduced order models, and compared them with the ones of a proportional-integral (PI) controller. In all the simulation runs, the initial condition:

$$n(r, 0) = 0.0, \quad c(0) = 990.0\,\mathrm{kg/m^3}$$

was used for the process model of Eqs. (1.1) and (1.2) and the finite-difference method with 1000 discretization points was used for its simulation. The crystal concentration, $\tilde{x}_0$ was considered to be the controlled output and the inlet solute concentration was chosen to be the manipulated input. Initially, the set-point tracking capability of the nonlinear controller was evaluated under nominal conditions for a 0.5 increase in the value of the set-point.

Fig. 2 shows the closed-loop output (left plot) and manipulated input (right plot) profiles obtained by using the nonlinear controller (solid lines). For the sake of comparison, the corresponding profiles under PI control are also included (dashed lines); the PI controller was tuned so that the closed-loop output response exhibits the same level of overshoot to one of the closed-loop outputs under nonlinear control. Clearly, the nonlinear controller drives the controlled output to its new set-point value in a significantly shorter time than the one required

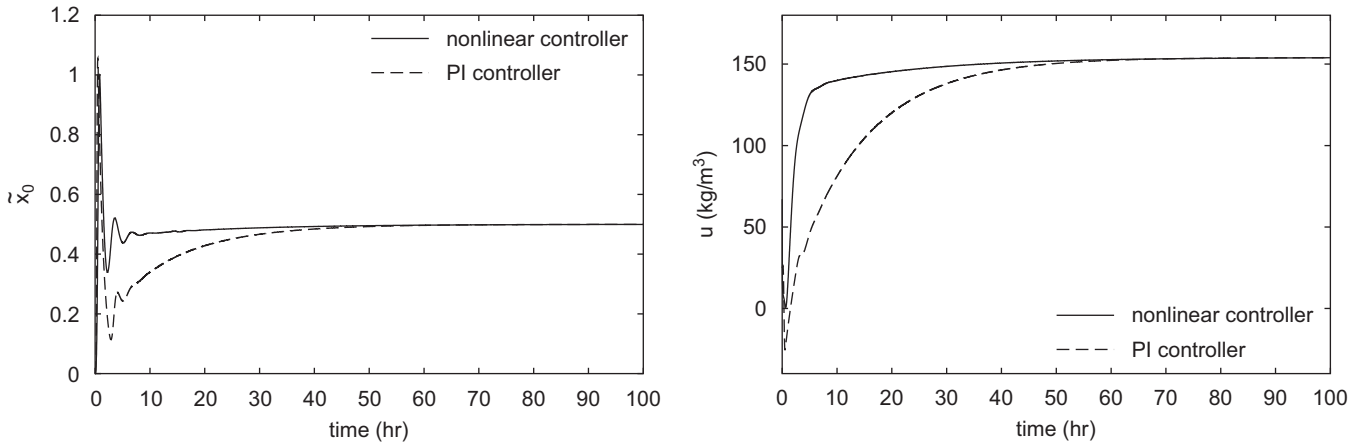

Fig. 2. Closed-loop output (left) and manipulated input (right) profiles under nonlinear and PI control, for a 0.5 increase in the set-point ($\tilde{x}_0$ is the controlled output) (Chiu and Christofides, 1999).

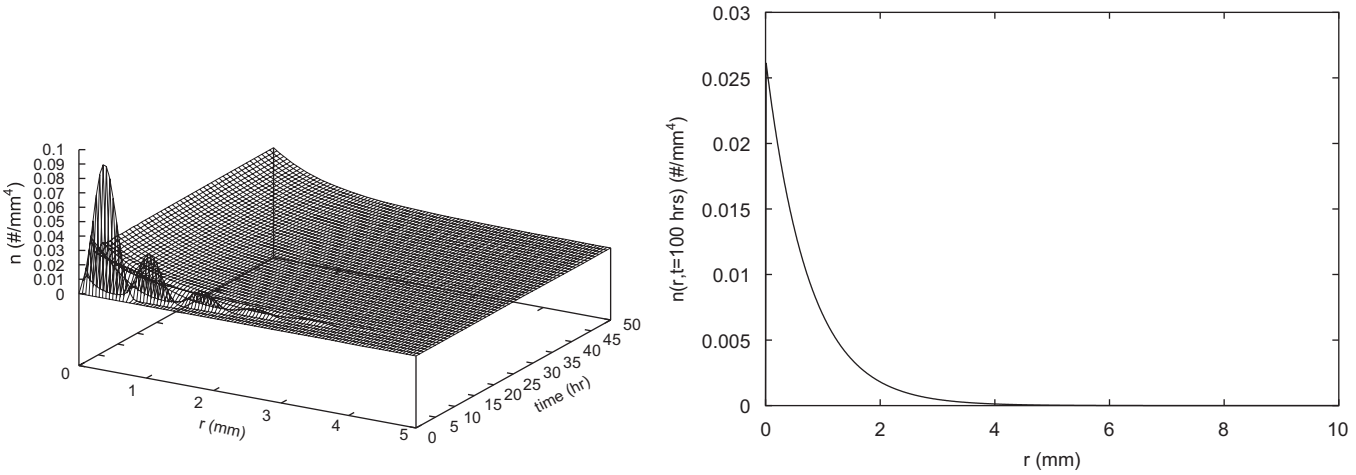

Fig. 3. Profile of evolution of CSD (left) and final steady-state CSD (right) under nonlinear control ($\tilde{x}_0$ is the controlled output) (Chiu and Christofides, 1999).

by the PI controller, while both controlled outputs exhibit very similar overshoot. For the same simulation run, the evolution of the closed-loop profile and the final steady-state profile of the CSD are shown in Fig. 3. An exponentially decaying CSD is obtained at the steady-state. The reader may refer to Chiu and Christofides (1999) for extensive simulation results.

2.4.2. Hybrid predictive control

In addition to handling nonlinear behavior, an important control problem is to stabilize the crystallizer at an unstable steady-state (which corresponds to a desired PSD) using constrained control action. Currently, the achievement of high performance, under control and state constraints, relies to a large extent on the use of model predictive control (MPC) policies. In this approach, a model of the process is used to make predictions of the future process evolution and compute control actions, through repeated solution of constrained optimization problems, which ensure that the process state variables satisfy the imposed limitations. However, the ability of the available model predictive controllers to guarantee closed-loop stability and enforce constraint satisfaction is dependent on the assumption of feasibility (i.e., existence of a solution) of the constrained optimization problem. This limitation strongly impacts the practical implementation of the MPC policies and limits the a priori (i.e., before controller implementation) characterization of the set of initial conditions, starting from where the constrained optimization problem is feasible and closed-loop stability is guaranteed. This problem typically results in the need for extensive closed-loop simulations and software verification (before on-line implementation) to search over the whole set of possible initial operating conditions that guarantee stability. This in turn can lead to prolonged periods for plant commissioning. Alternatively, the lack of a priori knowledge of the stabilizing initial conditions may necessitate limiting process operation within a small conservative neighborhood of the desired set-point in order to avoid extensive testing and simulations. Given the tight product quality specifications, however, both of these two remedies can impact negatively on the efficiency and profitability of the process by limiting its operational flexibility. Lyapunov-based analytical

control designs allow for an explicit characterization of the constrained stability region (El-Farra and Christofides, 2001, 2003; Lin and Sontag, 1991), however, their closed-loop performance properties, cannot be transparently characterized.

To overcome these difficulties, we recently developed (El-Farra et al., 2004) a hybrid predictive control structure that provides a safety net for the implementation of predictive control algorithms. The central idea is to embed the implementation of MPC within the stability region of a bounded controller and devise a set of switching rules that orchestrate the transition from MPC to the bounded controller in the event that MPC is unable to achieve closed-loop stability (e.g., due to inappropriate choice of the horizon length, infeasibility or computational difficulties). Switching between the two controllers allows reconciling the tasks of optimal stabilization of the constrained closed-loop system (through MPC) with that of computing a priori the set of initial conditions, for which closed-loop stability is guaranteed (through Lyapunov-based (El-Farra and Christofides, 2001, 2003) nonlinear bounded control).

We demonstrated the application of the hybrid predictive control strategy to the continuous crystallizer of Eqs. (1.1) and (1.2). The control objective was to suppress the oscillatory behavior of the crystallizer and stabilize it at an unstable steady-state that corresponds to a desired PSD by manipulating the inlet solute concentration. To achieve this objective, measurements or estimates of the first four moments and of the solute concentration are assumed to be available. Subsequently, the proposed methodology is employed for the design of the controllers using a low-order model constructed by using the method of moments. We compared the hybrid predictive control scheme, with an MPC controller designed with a set of stabilizing constraints and a Lyapunov-based nonlinear controller.

In the first set of simulation runs, we tested the ability of the MPC controller with the stability constraints to stabilize the crystallizer starting from the initial condition, $x(0) = [0.066\ 0.041\ 0.025\ 0.015\ 0.560]'$. The result is shown by the solid lines in Fig. 4(a)–(e) where it is seen that the predictive controller, with a horizon length of $T = 0.25$, is able to stabilize the closed-loop system at the desired equilibrium point. Starting from the initial condition $x(0)=[0.033\ 0.020\ 0.013\ 0.0075\ 0.570]'$, however, the MPC controller with the stability constraints yields no feasible solution. If the stability constraints are relaxed to make the MPC feasible, we see from the dashed lines in Fig. 4(a)–(e) that the resulting control action cannot stabilize the closed-loop system, and leads to a stable limit cycle. On the other hand, the bounded controller is able to stabilize the system from both initial conditions (this was guaranteed because both initial conditions lied inside the stability region of the controller). The state trajectory starting from $x(0) = [0.033\ 0.020\ 0.013\ 0.0075\ 0.570]'$ is shown in Fig. 4(a)–(e) with the dotted profile. This trajectory, although stable, presents slow convergence to the equilibrium as well as a damped oscillatory behavior that the MPC does not show when it is able to stabilize the system.

When the hybrid predictive controller is implemented from the initial condition $x(0)=[0.033\ 0.020\ 0.013\ 0.0075\ 0.570]'$, the supervisor detects initial infeasibility of MPC and implements the bounded controller in the closed-loop. As the closed-loop states evolve under the bounded controller and get closer to the desired steady-state, the supervisor finds (at $t = 5.8$ h) that the MPC becomes feasible and, therefore, implements it for all future times. Note that despite the "jump" in the control action profile as we switch from the bounded controller to MPC at $t = 5.8$ h (see the difference between dotted and dash-dotted profiles in Fig. 4(f)), the moments of the PSD in the crystallizer continue to evolve smoothly (dash-dotted lines in Fig. 4(a)–(e)). The supervisor finds that MPC continues to be feasible and is implemented in closed-loop to stabilize the closed-loop system at the desired steady-state. Compared with the simulation results under the bounded controller, the hybrid predictive controller (dash-dotted lines) stabilizes the system much faster, and achieves a better performance, reflected in a lower value of the performance index (0.1282 vs 0.1308). The manipulated input profiles for the three scenarios are shown in Fig. 4(f).

2.4.3. Predictive control of size distribution in a batch protein crystallizer

In batch crystallization, the main objective is to achieve a desired PSD at the end of the batch and satisfying state and control constraints during the whole batch run. Significant previous work has focused on CSD control in batch crystallizers, e.g., Rawlings et al. (1993) and Xie et al. (2001). In Miller and Rawlings (1994), a method was developed for assessing parameter uncertainty and studied its effects on the open-loop optimal control strategy, which maximized the weight mean size of the product. To improve the product quality expressed in terms of the mean size and the width of the distribution, an on-line optimal control methodology was developed for a seeded batch cooling crystallizer (Zhang and Rohani, 2003). In these previous works, most efforts were focused on the open-loop optimal control of the batch crystallizer, i.e., the optimal operating condition was calculated off-line and based on mathematical models. The successful application of such a control strategy relies, to a large extent, on the accuracy of the models. Furthermore, an open-loop control strategy may not be able to manipulate the system to follow the optimal trajectory because of the ubiquitous existence of modeling error. Motivated by this, we developed (Shi et al., 2006) a predictive control system to maximize the volume-averaged tetragonal lysozyme crystal size (i.e., μ_4/μ_3 where μ_3, μ_4 are the third and fourth moments of the crystal size distribution; see Eq. (2.11)) by manipulating the jacket temperature, T_j. The principle moments are calculated from the on-line measured CSD, n, which can be obtained by measurement techniques such as the laser light scattering method. The concentration and crystallizer temperature are also assumed to be measured in real time. In the closed-loop control structure, a reduced-order moments model was used within the predictive controller for the purpose of prediction. The main idea is to use this model to obtain a prediction of the state of the process at the end of the batch operation, t_f, from the current measurement at time t. Using this prediction, a cost function that depends on this value is minimized subject to a set

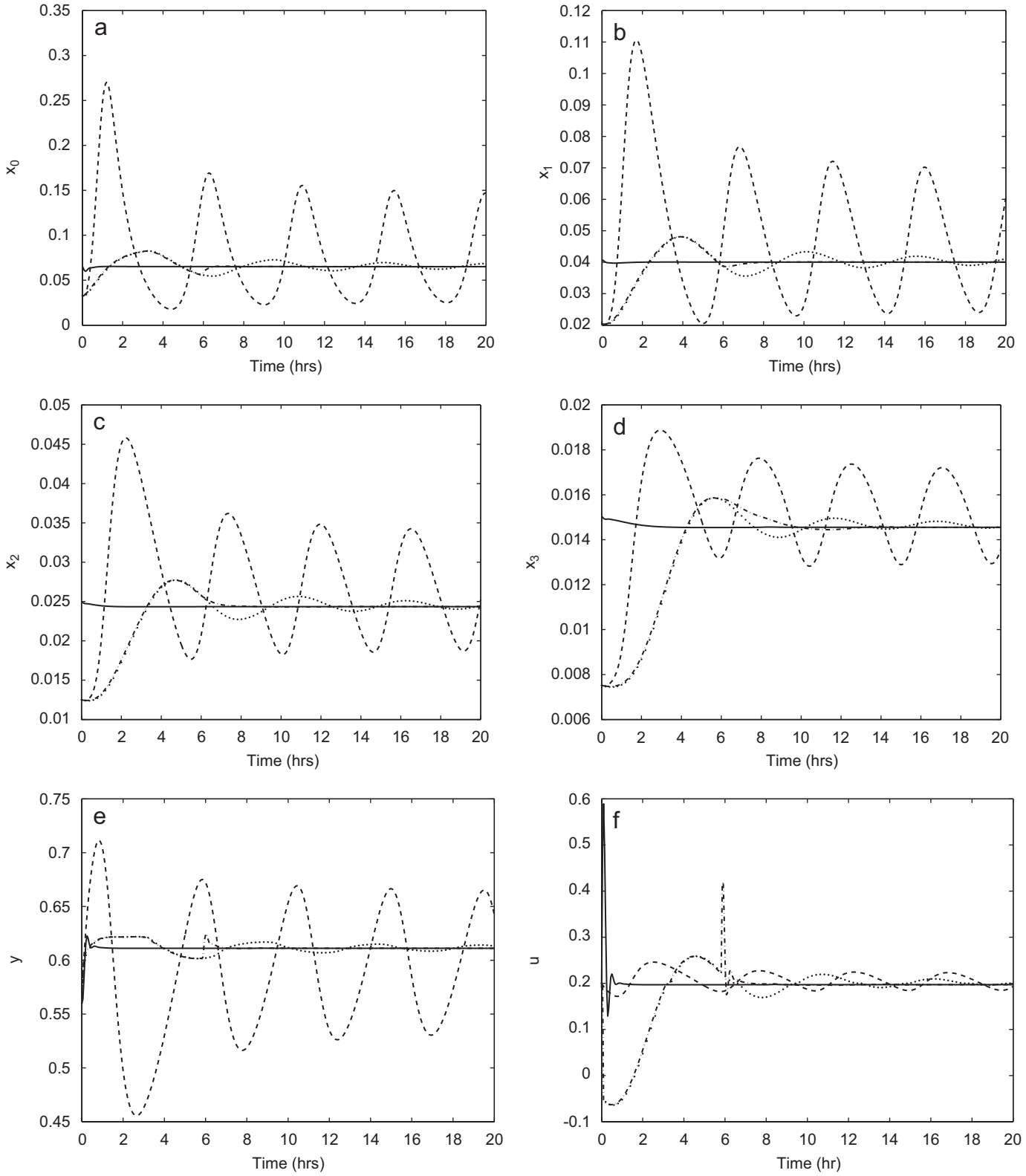

Fig. 4. Continuous crystallizer example: closed-loop profiles of the dimensionless crystallizer moments (a)–(d), the solute concentration in the crystallizer (e) and the manipulated input (f) under MPC with stability constraints (solid lines), under MPC without stability constraints (dashed lines), under the bounded controller (dotted lines), and using the hybrid predictive controller (dash-dotted lines) (Shi et al., 2006). Note the different initial states.

of operating constraints. Manipulated input limitations, specifications of supersaturation and crystallizer temperature are incorporated as input and state constraints on the optimization problem. The optimization profile computes the profile of the manipulated input T_j from the current time until the end of the batch operation interval, then the current value of the computed input is implemented on the process, and the optimization problem is resolved and the input is updated each time a new measurement is available (receding horizon control strategy). The optimization problem that is solved at each sampling instant takes the following form:

$$\min_{T_j} \quad -\frac{\mu_4(t_f)}{\mu_3(t_f)},$$

$$\text{s.t.} \quad \frac{\mathrm{d}\mu_0}{\mathrm{d}t} = k_a C \exp\left(-\frac{k_b}{\sigma^2}\right),$$

$$\frac{\mathrm{d}\mu_i}{\mathrm{d}t} = \mathrm{i}k_g \sigma^g \mu_{i-1}(t), \quad i = 1, \ldots, 4,$$

$$\frac{\mathrm{d}C}{\mathrm{d}t} = -24\rho k_v k_g \sigma^g \mu_2(t),$$

$$\frac{\mathrm{d}T}{\mathrm{d}t} = -\frac{UA}{MC_p}(T - T_j),$$

$$T_{\min} \leqslant T \leqslant T_{\max},$$

$$T_{j\min} \leqslant T_j \leqslant T_{j\max},$$

$$\sigma_{\min} \leqslant \sigma \leqslant \sigma_{\max},$$

$$\left\| \frac{\mathrm{d}C_s}{\mathrm{d}t} \right\| \leqslant k_1, \tag{2.12}$$

$$n(0, t) \leqslant n_{\text{fine}}, \quad \forall t \geqslant t_f/2, \tag{2.13}$$

where $T_{\min}$ and $T_{\max}$ are the constraints on the crystallizer temperature, T, and are specified as 4 and 22 °C, respectively. $T_{j\min}$ and $T_{j\max}$ are the constraints on the manipulated variable, T_j, and are specified as 3 and 22 °C, respectively. The constraints on the supersaturation σ are $\sigma_{\min} = 1.73$ and $\sigma_{\max} = 2.89$. The constant, k_1 (chosen to be 0.065 mg/ml min) specifies the maximum rate of change of the saturation concentration C_s. n_{fine} is the largest allowable number of nuclei at any time instant during the second half of the batch run, and is set to $5/\mu$m ml. In the simulation, the sampling time is 5 min, while the batch process time t_f is 24 h. The optimization problem is solved using sequential quadratic programming (SQP). A second-order accurate finite-difference scheme with 3000 discretization points is used to obtain the solution of the population balance model of Eq. (1.3). Referring to the predictive control formulation of Eq. (2.13), it is important to note the following: Previous work has shown that the objective of maximizing the volume-averaged crystal size can result in a large number of fines in the final product (Ma et al., 2002). To enhance the ability of the proposed predictive control strategy to maximize the performance objective while avoiding the formation of a large number of fines in the final product, the predictive controller of Eq. (2.13) includes a constraint on the number of fines present in the final product. Specifically, the constraint of Eq. (2.13), by restricting the number of nuclei formed at any time instant during the second half of the batch run limits the fines in the final product. Note that predictive control without constraint on fines can result in a product with a large number of fines (see Fig. 5(a)) which is undesirable. The implementation of the predictive controller with the constraint of Eq. (2.13), designed to reduce the fines in the product, results in a product with much less fines while still maximizing the volume-averaged crystal size (see Fig. 5(b)). The reader may refer to Shi et al. (2005, 2006) for further results on the performance of the predictive controller and comparisons with the performance of two other open-loop control strategies, constant temperature control (CTC) and constant supersaturation control (CSC).

2.4.4. Fault-tolerant control of particulate processes

Compared with the significant and growing body of research work on control of particulate processes, the problem of designing fault-tolerant control systems for particulate processes has not received much attention. This is an important problem given the vulnerability of automatic control systems to faults (e.g., malfunctions in the control actuators, measurement sensors or process equipment), and the detrimental effects that such faults can have on the process operating efficiency and product quality. Given that particulate processes play a key role in a wide range of industries (e.g., chemical, food and pharmaceutical) where the ability to consistently meet stringent product specifications is critical to the product utility, it is imperative that systematic methods for the timely diagnosis and handling of faults be developed to minimize production losses that could result from operational failures.

Motivated by these considerations, recent research efforts have started to tackle this problem by bringing together tools from model-based control, infinite-dimensional systems, fault diagnosis and hybrid systems theory. For particulate processes modeled by population balance equations with control constraints, actuator faults and a limited number of process measurements, a fault-tolerant control architecture that integrates model-based fault detection, feedback and supervisory control has recently been developed in El-Farra and Giridhar (2007). The architecture, which is based on reduced-order models that capture the dominant dynamics of the particulate process, consists of a family of control configurations, together with a fault detection filter and a supervisor. For each configuration, a stabilizing output feedback controller with well-characterized stability properties is designed through combination of a state feedback controller and a state observer that uses the available measurements of the principal moments of the PSD and the continuous-phase variables to provide appropriate state estimates. A fault detection filter that simulates the behavior of the fault-free, reduced-order model is then designed, and its discrepancy from the behavior of the actual process state estimates is used as a residual for fault detection. Finally, a switching law based on the stability regions of the constituent control configurations is derived to reconfigure the control

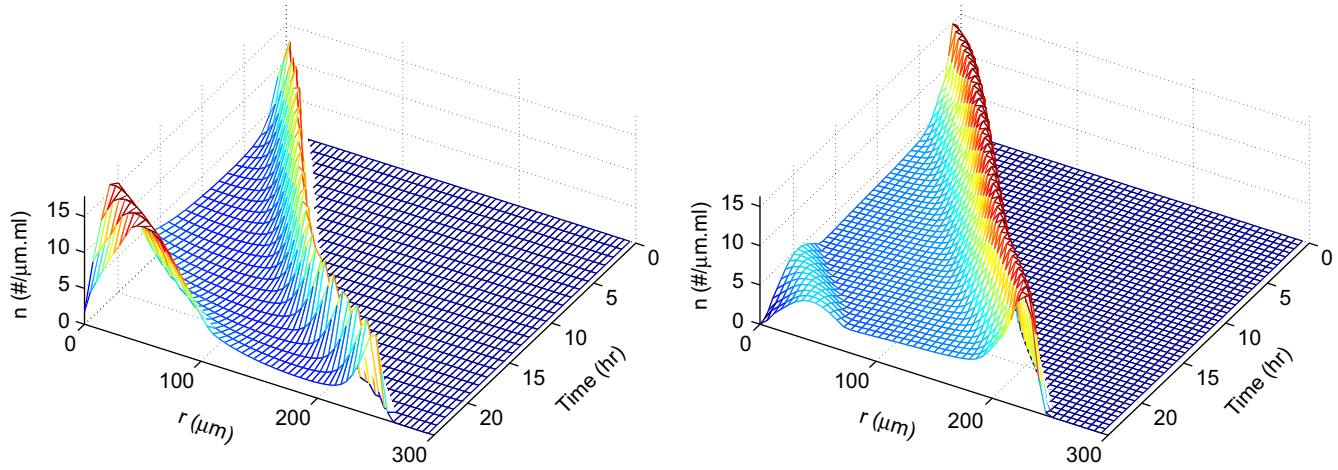

Fig. 5. Evolution of PSD under (left) predictive control without constraint on fines, and (right) predictive control with constraint on fines (Shi et al., 2005).

system in a way that preserves closed-loop stability in the event of fault detection. Appropriate fault detection thresholds and control reconfiguration criteria that account for model reduction and state estimation errors were derived for the implementation of the control architecture on the particulate process. The methodology was successfully applied to a continuous crystallizer example where the control objective was to stabilize an unstable steady-state and achieve a desired CSD in the presence of constraints and actuator faults.

In addition to the synthesis of actuator fault-tolerant control systems for particulate processes, recent research efforts have also investigated the problem of preserving closed-loop stability and performance of particulate processes in the presence of sensor data losses (Gani et al., 2007). Typical sources of sensor data losses include measurement sampling losses, intermittent failures associated with measurement techniques, as well as data packet losses over transmission lines. In this work, two representative particulate process examples—a continuous crystallizer and a batch protein crystallizer—were considered. In both examples, feedback control systems were first designed on the basis of low-order models and applied to the population balance models to enforce closed-loop stability and constraint satisfaction. Subsequently, the robustness of the control systems in the presence of sensor data losses was investigated using a stochastic formulation developed in Mhaskar et al. (2007) that models sensor failures as a random Poisson process. In the case of the continuous crystallizer, a Lyapunov-based nonlinear output feedback controller was designed and shown to stabilize an open-loop unstable steady-state of the population balance model in the presence of input constraints. Analysis of the closed-loop system under sensor malfunctions showed that the controller is robust with respect to significant sensor data losses, but cannot maintain closed-loop stability when the rate of data losses exceeds a certain threshold. In the case of the batch crystallizer, a predictive controller was designed to obtain a desired CSD at the end of the batch while satisfying state and input constraints. Simulation results showed how constraint modification in the predictive controller formulation can assist in achieving constraint satisfaction under sensor data losses.

2.4.5. Nonlinear control of aerosol reactors

The crystallization process examples discussed in the previous section share the common characteristic of having two independent variables (time and particle size). In such a case, order reduction, for example with the method of moments, leads to a set of ODEs in time as a reduced-order model. This is not the case, however, when three or more independent variables (time, particle size and space) are used in the process model. An example of such a process is the aerosol flow reactor presented in the Introduction. The complexity of the partial integro-differential equation model of Eq. (1.6) does not allow its direct use for the synthesis of a practically implementable nonlinear model-based feedback controller for spatially inhomogeneous aerosol processes. Therefore, we developed (Kalani and Christofides, 1999, 2000, 2002) a model-based controller design method for spatially inhomogeneous aerosol processes, which is based on the experimental observation that many aerosol size distributions can be adequately approximated by lognormal functions. The proposed control method can be summarized as follows:

(1) Initially, the aerosol size distribution is assumed to be described by a lognormal function and the method of moments is applied to the aerosol population balance model of Eq. (1.6) to compute a hyperbolic partial differential equation (PDE) system (where the independent variables are time and space) that describes the spatio-temporal behavior of the three leading moments needed to exactly describe the evolution of the lognormal aerosol size distribution.
(2) Then, nonlinear geometric control methods for hyperbolic PDEs (Christofides and Daoutidis, 1996) are applied to the resulting system to synthesize nonlinear distributed output feedback controllers that use process measurements at different locations along the length of the process to adjust the manipulated input (typically, wall temperature), in

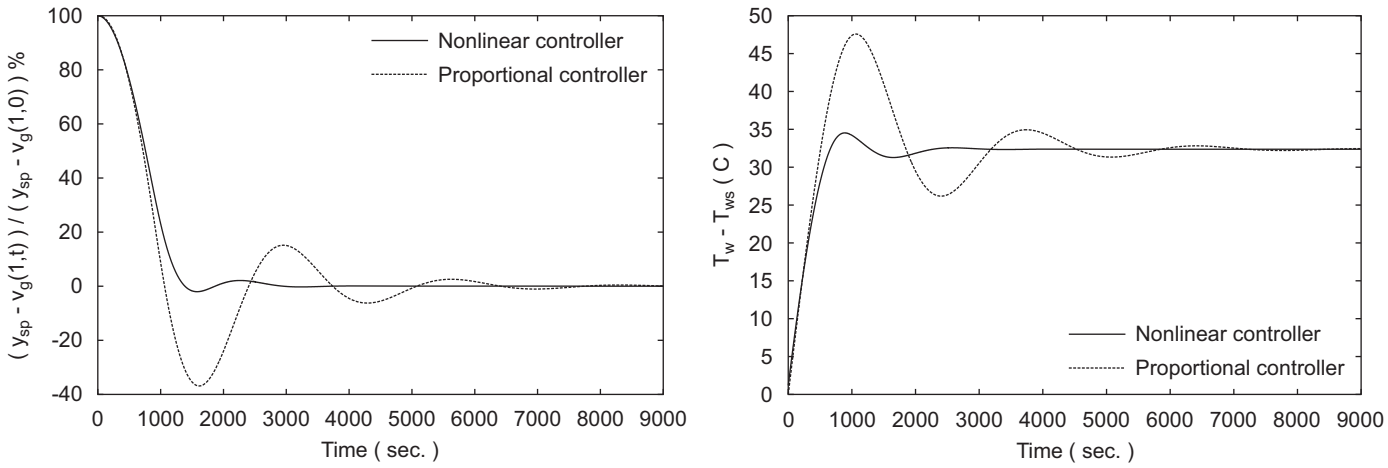

Fig. 6. Closed-loop profiles of scaled mean particle volume in the outlet of the reactor under proportional integral and nonlinear controllers (left). Manipulated input profiles for proportional integral and nonlinear controllers (right) (Kalani and Christofides, 1999).

order to achieve an aerosol size distribution with desired characteristics (e.g., geometric average particle volume).

We carried an application of this nonlinear control method to an aerosol flow reactor, including nucleation, condensation and coagulation, used to produce NH_4Cl particles (Kalani and Christofides, 1999) and a titania aerosol reactor (Kalani and Christofides, 2000). To provide a flavor of our results in the context of the aerosol process used to produce NH_4Cl particles, Fig. 6 (left plot—solid line) shows the profile of the controlled output which is the mean particle volume at the outlet of the reactor $v_g(1,t)$, while Fig. 6 (right plot—solid line) displays the corresponding profile of the manipulated input which is the wall temperature. The proposed nonlinear controller regulates successfully, $v_g(1,t)$ to its new set-point value. For the sake of comparison, we also implemented on the process a proportional integral controller; this controller was tuned so that the time which the closed-loop outputs need to reach the final steady-state is the same to one of the closed-loop outputs under nonlinear control. The profiles of the controlled output and manipulated input are shown in Fig. 6 (dashed lines show the profiles for the proportional integral controller). It is clear that the proposed nonlinear controller outperforms the proportional integral controller.

3. Multiscale modeling and control of thermal spray coating processes

While most of the researches on model-based control of particulate processes has focused on processes described by population balance models, there are many processes that involve coupling of a continuous phase and a particulate phase which are not naturally described by population balances. An example is the high-velocity oxygen-fuel (HVOF) thermal spray process which is a particulate deposition process in which the particles are first heated and propelled in a reacting gas stream and are then deposited and deformed on the substrate, resulting in a layer of lamellar coating. HVOF thermal spray is a versatile technology widely used in aerospace, automobile and chemical industries to deposit coatings on a substrate in order to extend product life, increase performance and reduce production and maintenance costs. Examples of thermal spray coatings are WC/Co-based wear resistant coatings for drilling tools, YSZ-based thermal barrier coatings for blades in internal engines and Ni-based corrosion resistant coatings in chemical reactors. YSZ coatings prepared by plasma spray are also used as electrolytes in solid oxide fuel cells.

While the operation of the HVOF thermal spray process has been largely dependent on design of experiments (e.g., de Villiers Lovelock et al., 1998; Gil and Staia, 2002; Gourlaouen et al., 2000; Hanson et al., 2002; Hearley et al., 2000; Lih et al., 2000; Lugscheider et al., 1998), model-based process optimization and control provides a more efficient tool in the development of this process because the developed fundamental understanding of the underlying physicochemical behavior of the process, embedded in a process model, can be utilized. The major challenge on this problem was the development of multiscale models linking the macroscopic scale process behavior (i.e., gas dynamics and particle inflight behavior) and the microscopic scale process characteristics (evolution of coating microstructure), and the integration of models, measurements and control theory to develop measurement/model-based control strategies. The multiscale feature of the HVOF thermal spray process is shown in Fig. 7. The microstructure of sprayed coatings results from the deformation, solidification and sintering of the deposited particles, which are dependent on the substrate properties (e.g., substrate temperature) as well as the physical and chemical states (e.g., temperature, velocity, melting ratio, and oxidant content, etc.) of the particles at the point of impact on the substrate. On the other hand, the particle inflight behavior, however, is coupled with the gas dynamics, which can be manipulated by adjusting operating conditions such as the gas flow rate of fuel, oxygen and cooling air. While the macroscopic thermal/flow field can be readily described

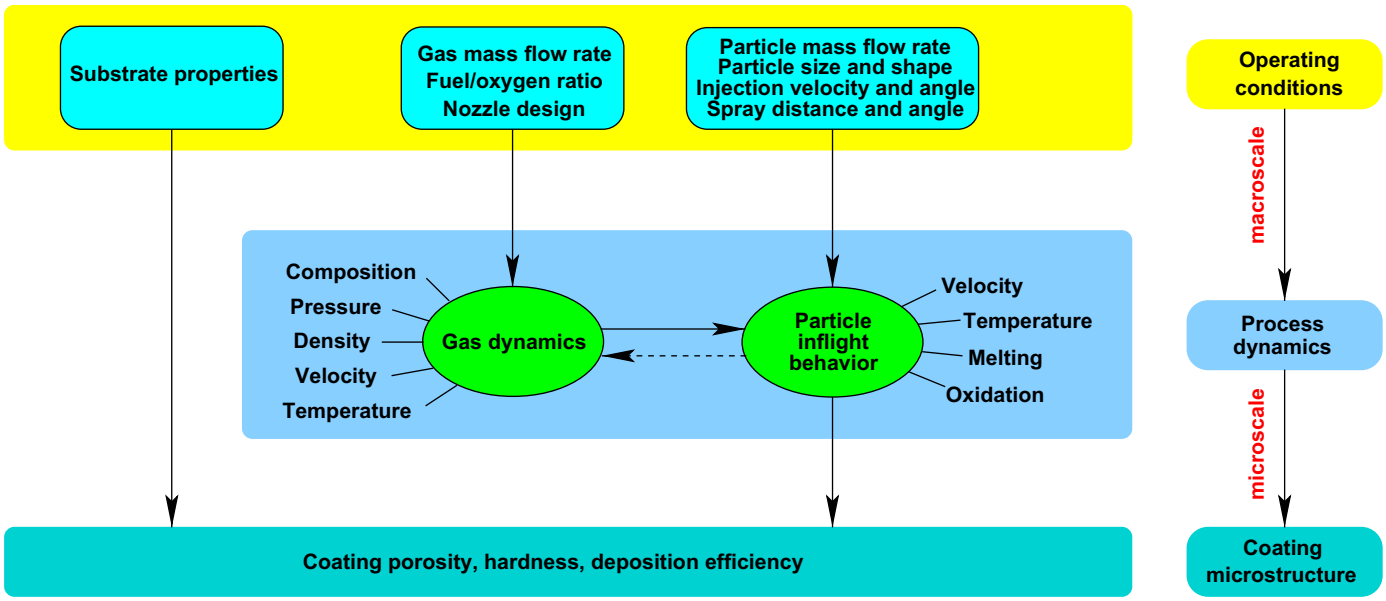

Fig. 7. Multiscale feature of the HVOF thermal spray process (Li et al., 2004a).

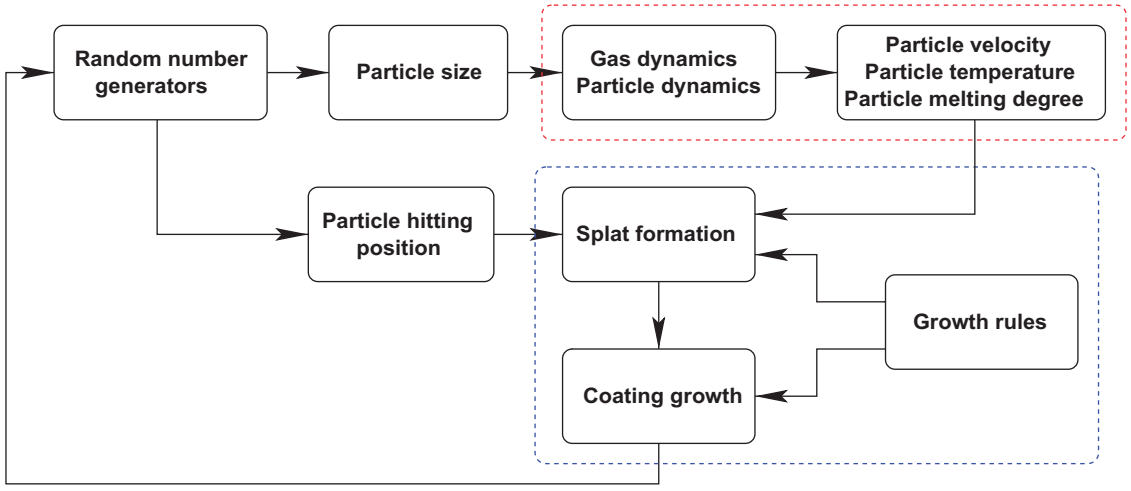

Fig. 8. Multiscale modeling of the HVOF thermal spray process (Li et al., 2004a; Shi et al., 2004).

by continuum type differential equations governing the compressible two-phase flow, the process of particle deposition is stochastic and discrete in nature, and thus it can be best described by stochastic simulation methods (Knotek and Elsing, 1987). By manipulating macro-scale operating conditions such as gas feed flow rates and spray distance, one can control the coating microstructure which determines the coating mechanical and physical properties.

In the past several years, we developed a computational framework for the HVOF thermal spray processing of nanostructured coatings (Li and Christofides, 2003, 2004, 2005, 2006; Li et al., 2004a,b, 2005; Shi et al., 2004). The multiscale process model encompasses gas dynamics of the supersonic reacting flow, evolution of particle velocity, temperature and molten state during flight, and stochastic growth of coating microstructure, as shown in Fig. 8. Parametric analysis based on the multiscale model pointed out the coating microstructure is highly dependent on particle velocity, temperature and molten state at impact on substrate, which can be almost independently adjusted by pressure in the combustion chamber and fuel/oxygen ratio. A model-based control scheme was developed based on the gas-phase measurement and the estimation of particle properties through the dynamic particle inflight model and was designed to control the particle velocity and melting ratio at impact by adjusting the flow rate of cooling air, oxygen and fuel, through which the pressure and fuel/oxygen can be independently adjusted. The multivariable feedback control system was applied to a detailed mathematical model of the process and the closed-loop simulations showed that the proposed controller was effective in set-point tracking and also robust with respect to disturbances in the processing environment, such as spray distance and particle injection velocity, and variations in

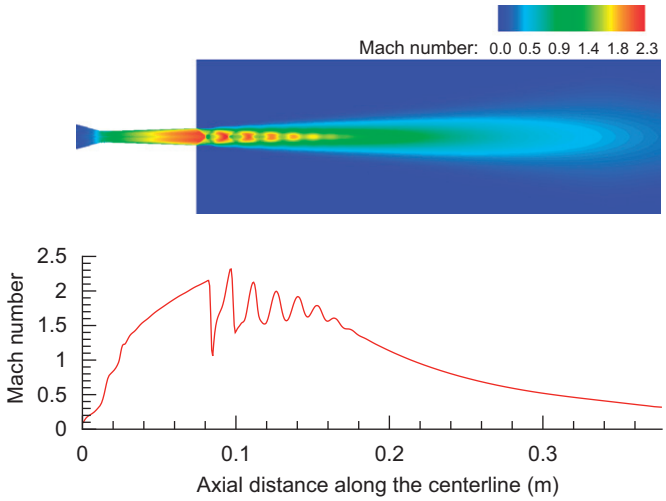

Fig. 9. Centerline Mach number and its contour in the internal and external flow field (Li and Christofides, 2005).

powder size distribution. In the remainder of this section, we will provide an overview of the progress in this area.

The gas dynamics in the HVOF thermal spray process depend on the combustion process and involve subsonic–supersonic–subsonic transitions. We developed both a computational fluid dynamic (CFD) model (Li and Christofides, 2005, 2006) and a simplified quasi-one-dimensional model derived from the conservation of mass, momentum and energy (Li and Christofides, 2003; Li et al., 2004a). The numerical study demonstrated that the chemical energy is converted to thermal energy of the gas through combustion, which is then partially converted to kinetic energy through the convergent-divergent nozzle flow. The evolution of Mach number in the entire flow field is shown in Fig. 9. We see clearly a constant increase in the Mach number in the internal flow field, which suggests a conversion of thermal energy into kinetic energy. In the convergent section of the nozzle, the flow is subsonic. At the throat of the nozzle, where the flow is choked, the Mach number is close to 1. The gas is accelerated to supersonic velocity in the divergent section of the nozzle and reaches a Mach number around 2 at the exit of the nozzle. Outside of the thermal spray gun, the jet adjusts to the ambient pressure through a series of compression and expansion waves and subsequently both gas velocity and temperature decay due to the entrainment of the surrounding air.

The particle trajectories and temperature histories in the gas field are computed by the following multiphase momentum and heat transfer equations (Li et al., 2004a):

$$m_p \frac{\mathrm{d}v_p}{\mathrm{d}t} = \frac{1}{2} C_D \rho_g A_p (v_g - v_p)|v_g - v_p|,$$

$$\frac{\mathrm{d}x_p}{\mathrm{d}t} = v_p,$$

$$m_p c_{p_p} \frac{\mathrm{d}T_p}{\mathrm{d}t} = \begin{cases} hA'_p(T_g - T_p) + S_h & (T_p \neq T_m), \\ 0 & (T_p = T_m), \end{cases}$$

$$\Delta H_m m_p \frac{\mathrm{d}f_p}{\mathrm{d}t} = \begin{cases} hA'_p(T_g - T_p) + S_h & (T_p = T_m), \\ 0 & (T_p \neq T_m), \end{cases} \tag{3.14}$$

where m_p is the mass of the particle, t the time, v_p the axial velocity of the particle, A_p the projected area of the particle on the plane perpendicular to the flow direction, ρ_g the density of the gas, C_D the drag coefficient, x_p the position of the particle, T_p the temperature of the particle, A'_p the surface area of the particle, T_m the melting point of the particle, ΔH_m the enthalpy of melting, f_p the mass fraction of melted part in the particle ($0 \leqslant f_p \leqslant 1$) and S_h the source term including heat transfer due to radiation ($\varepsilon\sigma A'_p(T_g^4 - T_p^4)$) and oxidation. The above equations describing particle velocity, position, temperature and degree of particle melting are solved by fourth order Runge–Kutta method. In all the mathematical formulas, the thermodynamic and transport properties of each species and product mixture are calculated using formulas provided in Gordon and McBride (1994). A more comprehensive particle model that accounts for the multi-dimensional particle tracking, random fluctuation in the gas field and injection distribution in the particle delivery tube is developed in Li and Christofides (2006).

It is shown that particles are involved in complicated physical processes. The particle velocity and temperature typically increase first and decrease in the flow field, which is consistent with experimental observations (Legoux et al., 2002; Swank et al., 1994). In particular, small particles might be melted during flight and be solidified later (Li et al., 2004a). Due to the interplay between the difference in the momentum/thermal inertia of particles of different sizes and the decay of the gas velocity and temperature outside of the thermal spray gun, there is usually a peak in the profile of impact temperature or velocity as a function of particle size, which occurs at particle diameter around 10–20 μm. However, because particles might take different trajectories due to different injection locations in the carrier nitrogen at the entrance of the thermal spray gun as well as the turbulent fluctuation in the gas flow and thermal fields, particles of the same size might still achieve different velocities and temperatures at impact on the substrate (Li and Christofides, 2006), which partially explains the experimental observations (e.g., Zhao et al., 2004)). While the simulation indicates that there is a spatial distribution of particle velocity and temperature on the substrate, this effect is generally minimal as compared to particle size (Li and Christofides, 2006).

The particle velocity, temperature and molten state of particles following a specific size distribution function are inputs to a model describing the evolution of coating microstructure (Shi et al., 2004). In this stochastic model, the coating growth process is described as a sequence of independent discrete events of each individual particle landing on or bouncing off the previously formed coating layer, and a slice of the coating that is perpendicular to the substrate is simulated based on a two-dimensional lattice with rectangular grid elements. Any lattice that is empty represents a pore (or a part of a pore) and otherwise it is a part of the coating. The model includes several scenarios that may exist in the coating growth process and several different rules are set to guide the simulator whether the particle flattens, breaks, attaches or bounces off on the

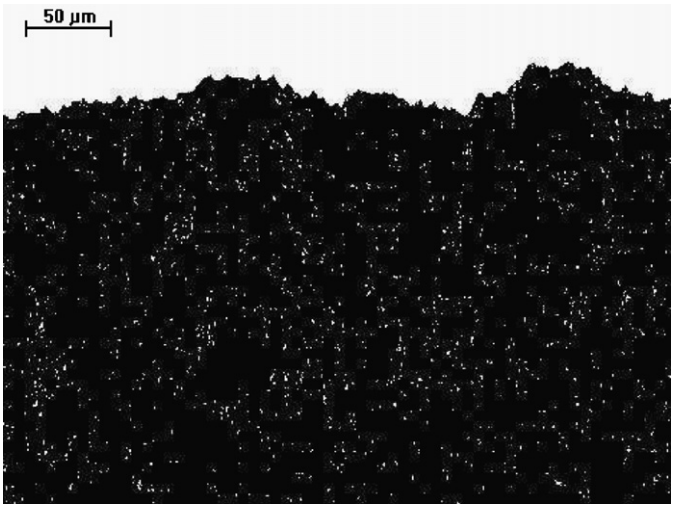

Fig. 10. Pore distribution in the thermal spray coating (Shi et al., 2004).

substrate surface and how each event affects the coating growth. A typical simulated pore distribution is shown in Fig. 10. Parametric analysis based on the stochastic coating growth model indicates that a moderately high particle temperature and melting degree reduce the coating porosity and increase the deposition efficiency because less particles are bounced off the substrate. Moreover, a high particle velocity improves both coating porosity and deposition efficiency because a large flatten ratio can be achieved. These conclusions are consistent with experimental observations (e.g., Hanson and Settles, 2003; Legoux et al., 2002).

In order to find a way to control the particle velocity and temperature, parametric analysis on the gas phase is made which shows that the particle velocity and temperature can be almost independently adjusted by pressure in the combustion chamber and fuel/oxygen ratio (i.e., equivalence ratio). As shown in Fig. 11, the drag force for particle motion, which is approximately proportional to the gas momentum flux (ρv_g^2), is a linear function of the chamber pressure. However, the temperature increases slightly as the pressure increases. On the other hand, the gas temperature varies with the fuel/oxygen ratio with an optimal value slightly larger than the stoichiometric value (or fuel rich conditions) and a change in the fuel/oxygen ratio with a fixed chamber pressure has little effect on the gas momentum flux.

Based on the above control relevant analysis, the control problem was formulated as one of the regulating volume-based averages of the temperature and velocity of the particles at the point of impact on the substrate by manipulating the oxygen/fuel ratio and the combustion chamber pressure with available particle velocity and temperature measurements. Two PI controllers were used to control the process (Li and Christofides, 2004). A modified control system that aims to adjust the particle velocity, temperature and melting degree through direct manipulation of the mass flow rate of fuel and oxygen was also proposed (Li et al., 2004a, 2005) because the gas flow rate is easier to manipulate than the pressure in

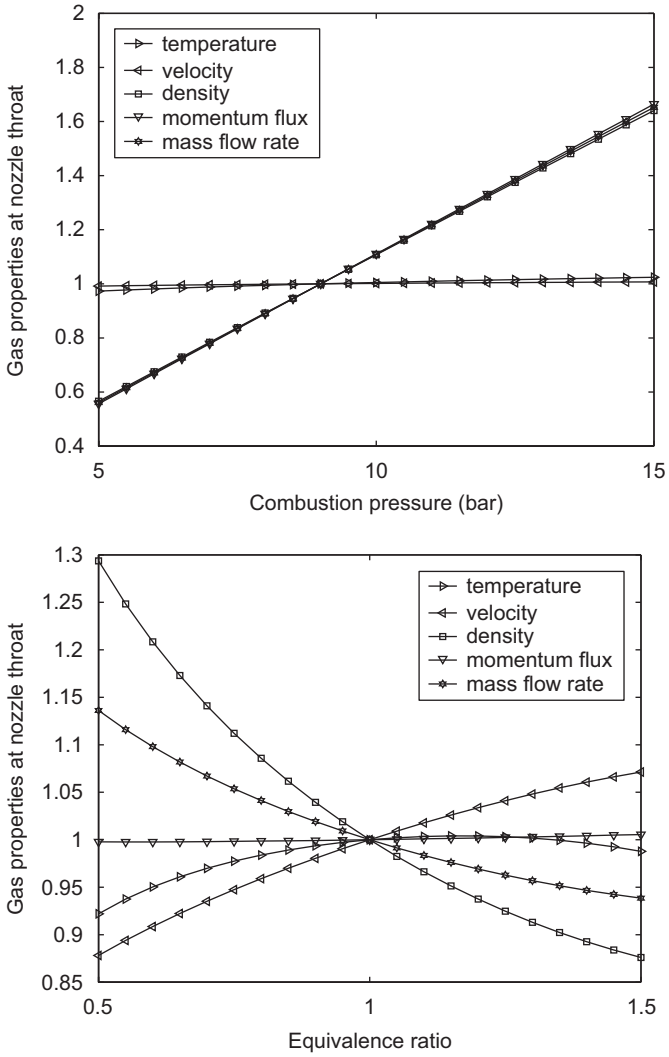

Fig. 11. Influence of pressure and fuel/oxygen ratio on gas momentum flux and gas temperature (Li et al., 2004a).

practice. Due to the fact that the particle melting degree is hard to measure, a model-based control scheme that incorporates the estimation of particle properties through the gas-phase measurement and particle dynamics was also developed (Li et al., 2004b). A representative closed-loop simulation is shown in Fig. 12 which indicates that the controller is effective in achieving set-point tracking. It was also demonstrated in Li et al. (2004b) that the robustness of closed-loop system in the presence of disturbances such as variations in spray distance and powder size distribution is excellent, which strongly motivates the implementation of real-time control systems on industrial HVOF thermal spray processes.

4. Future research challenges

While significant work has been done on control of particulate processes over the last 10 years, there is a number of emerging applications within the areas of nanotechnology, advanced materials processing and energy where control of

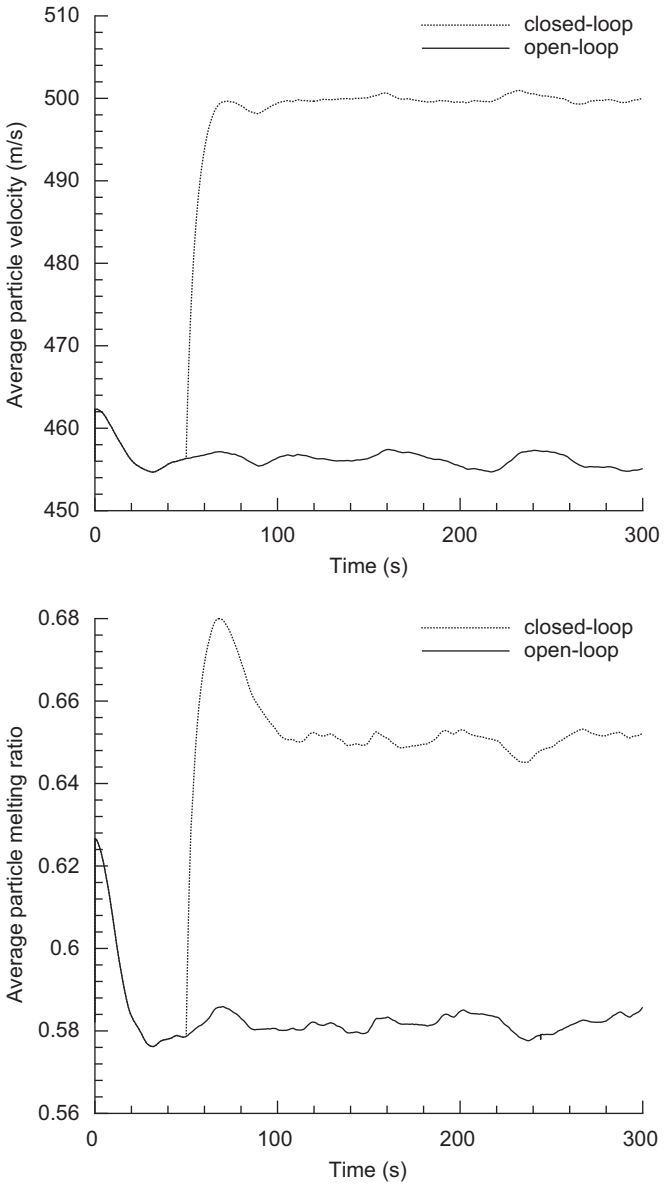

Fig. 12. Profiles of controlled outputs (average particle velocity and average particle melting ratio) and manipulated inputs (gas flow rates of propylene and oxygen) under the request of set-point change in the average particle velocity and average particle melting ratio (Li et al., 2004b).

PSD could provide the enabling technology for optimizing the performance and robustness of key processes. For example, significant interest has been generated recently in the field of nanoparticle synthesis and processing which has potential applications in the manufacture of catalysts, coatings, sensors, membranes and ceramics. The nanostructured materials fabricated by the processing of nanoparticles (characterized by a grain size less than 100 nm) exhibit superior qualities to conventional counterparts due to larger surface area to volume ratio and larger grain boundaries/interfaces. Representative examples include nanostructured titania coatings prepared by aerosol-assisted chemical vapor deposition, nanostructured tin oxide sensors prepared by flame spray pyrolysis, and nanostructured solid oxide fuel cells prepared by laser reactive deposition, etc. In these aerosol-based nanoparticle synthesis and deposition processes, the PSD plays an important role in the property of the final product and should be precisely controlled. To describe the evolution of the PSD in these processes, a general aerosol dynamic equation including condensation, nucleation, coagulation might be necessary and approaches such as the ones proposed in Kalani and Christofides (1999, 2000) might be followed for the PSD control in these processes.

In the area of hydrogen generation, it has been reported that the water splitting thermochemical cycle achieved through the metal/metal oxide redox reactions using solar energy is a promising route for high efficiency and safe hydrogen generation because the separation of H_2/O_2 is circumvented (Steinfeld, 2005). Recent efforts have reported a novel hydrogen generation process in which the formation of Zn nanoparticles and the in situ hydrolysis of hydrogen are integrated in a single tubular aerosol flow reactor (Weiss et al., 2005; Wegner et al., 2006). The high specific surface area provided by the Zn nanoparticles significantly enhances the heat/mass transfer and reaction rate, and thus the hydrogen yield (up to 70%). While it is obvious that a small particle size is beneficial for hydrogen yield, the development of a size control system for zinc hydrolysis remains an intellectually challenging problem.

In the semiconductor manufacturing industry, the particle removal becomes extremely critical as the chips become smaller and smaller. According to the International Technology Roadmap for Semiconductors, the “killer” particle size, defined as one-half of the gate length, was 40 nm in 2005 and is projected to reduce to 23 nm by the year 2010 (Semiconductor Industry Association, 2005). These particles are typically generated by gas-phase nucleation. The same problem occurs in the glass coating industry where particles generated from gas-phase nucleation can deposit and adhere to the transport channels, thereby restricting flow and reducing run length due to the necessity to clean the coating apparatus. The main challenge in this area is to develop computational models to predict formation, kinetics and transport of particles as a function of the process flow and thermal conditions and to identify the dominant chemical clustering pathways and limiting growth mechanisms. A high-fidelity model will not only provide guidelines for process and equipment design but also facilitate the development of model-based online diagnosis and control system for particle contamination control. The reader may refer to Christofides et al. (2007) for a detailed discussion on future problems on control of particulate processes.

Acknowledgments

Financial support from the NSF (ITR), CTS-0325246 and the Office of Naval Research (2001 Young Investigator Award) is gratefully acknowledged. The authors would like to thank Dr. David Muñoz de la Peña for providing valuable comments on the structure and content of the manuscript.

References

Braatz, R.D., Hasebe, S., 2002. Particle size and shape control in crystallization processes. In: Rawlings, J.B., et al. (Eds.), AIChE Symposium Series: Proceedings of the 6th International Conference on Chemical Process Control, 2002, pp. 307–327.

Chiu, T., Christofides, P.D., 1999. Nonlinear control of particulate processes. A.I.Ch.E. Journal 45, 1279–1297.

Chiu, T., Christofides, P.D., 2000. Robust control of particulate processes using uncertain population balances. A.I.Ch.E. Journal 46, 266–280.

Christofides, P.D., 2002. Model-based control of particulate processes. Particle Technology Series. Kluwer Academic Publishers, Netherlands, 2002.

Christofides, P.D., Chiu, T., 1997. Nonlinear control of particulate processes. In: AIChE Annual Meeting, paper 196a, Los Angeles, CA.

Christofides, P.D., Daoutidis, P., 1996. Feedback control of hyperbolic PDE systems. A.I.Ch.E. Journal 42, 3063–3086.

Christofides, P.D., Li, M.H., Mädler, L., 2007. Control of particulate processes: recent results and future challenges. Powder Technology 175, 1–7.

Daoutidis, P., Henson, M., 2001. Dynamics and control of cell populations. In: Proceedings of the 6th International Conference on Chemical Process Control, Tucson, AZ, pp. 308–325.

de Villiers Lovelock, H.L., Richter, P.W., Benson, J.M., Young, P.M., 1998. Parameter study of HP/HVOF deposited WC–Co coatings. Journal of Thermal Spray Technology 7, 97–107.

Dimitratos, J., Elicabe, G., Georgakis, C., 1994. Control of emulsion polymerization reactors. A.I.Ch.E. Journal 40, 1993–2021.

Doyle, F.J., Soroush, M., Cordeiro, C., 2002. Control of product quality in polymerization processes. In: Rawlings, J.B., et al. (Eds.), AIChE Symposium Series: Proceedings of the 6th International Conference on Chemical Process Control, pp. 290–306.

El-Farra, N.H., Christofides, P.D., 2001. Integrating robustness, optimality, and constraints in control of nonlinear processes. Chemical Engineering Science 56, 1–28.

El-Farra, N.H., Christofides, P.D., 2003. Bounded robust control of constrained multivariable nonlinear processes. Chemical Engineering Science 58, 3025–3047.

El-Farra, N.H., Giridhar, A., 2007. Detection and management of actuator faults in controlled particulate processes using population balance models, Chemical Engineering Science, doi: 10.1016/j.ces.2007.07.019.

El-Farra, N.H., Chiu, T., Christofides, P.D., 2001. Analysis and control of particulate processes with input constraints. A.I.Ch.E. Journal 47, 1849–1865.

El-Farra, N.H., Mhaskar, P., Christofides, P.D., 2004. Hybrid predictive control of nonlinear systems: method and applications to chemical processes. International Journal of Robust and Nonlinear Control 14, 199–225.

Friendlander, S.K., 2000. Smoke, Dust and Haze: Fundamentals of Aerosol Dynamics. second ed. Oxford University Press, New York, USA.

Gani, A., Mhaskar, P.,Christofides, P. D., 2007. Handling sensor malfunctions in control of particulate processes, Chemical Engineering Science, doi: 10.1016/j.ces.2007.07.020.

Gelbard, F., Seinfeld, J.H., 1978. Numerical solution of the dynamic equation for particulate processes. Journal of Computational Physics 28, 357–375.

Gil, L., Staia, M.H., 2002. Influence of HVOF parameters on the corrosion resistance of NiWCrBSi coatings. Thin Solid Films 420–421, 446–454.

Gordon, S., McBride, B.J., 1994. Computer Program for Calculation of Complex Chemical Equilibrium Compositions and Applications. NASA Reference Publication 1311, Lewis Research Center, Cleveland, OH, USA.

Gourlaouen, V., Verna, E., Beaubien, P., 2000. Influence of flame parameters on stainless steel coatings properties. In: Thermal Spray: Surface Engineering via Applied Research, Proceedings of the International Thermal Spray Conference, Montreal, QC, Canada, pp. 487–493.

Hanson, T.C., Settles, G.S., 2003. Particle temperature and velocity effects on the porosity and oxidation of an HVOF corrosion-control coating. Journal of Thermal Spray Technology 12, 403–415.

Hanson, T.C., Hackett, C.M., Settles, G.S., 2002. Independent control of HVOF particle velocity and temperature. Journal of Thermal Spray Technology 11, 75–85.

Hearley, J.A., Little, J.A., Sturgeon, A.J., 2000. The effect of spray parameters on the properties of high velocity oxy-fuel NiAl intermetallic coatings. Surface & Coatings Technology 123, 210–218.

Hulburt, H.M., Katz, S., 1964. Some problems in particle technology: a statistical mechanical formulation. Chemical Engineering Science 19, 555–574.

Jerauld, G.R., Vasatis, Y., Doherty, M.F., 1983. Simple conditions for the appearance of sustained oscillations in continuous crystallizers. Chemical Engineering Science 38, 1675–1681.

Kalani, A., Christofides, P.D., 1999. Nonlinear control of spatially-inhomogeneous aerosol processes. Chemical Engineering Science 54, 2669–2678.

Kalani, A., Christofides, P.D., 2000. Modeling and control of a titania aerosol reactor. Aerosol Science and Technology 32, 369–391.

Kalani, A., Christofides, P.D., 2002. Simulation, estimation and control of size distribution in aerosol processes with simultaneous reaction, nucleation, condensation and coagulation. Computers & Chemical Engineering 26, 1153–1169.

Knotek, O., Elsing, R., 1987. Monte carlo simulation of the lamellar structure of thermally sprayed coatings. Surface & Coatings Technology 32, 261–271.

Larsen, P.A., Rawlings, J.B., Ferrier, N.J., 2006. An algorithm for analyzing noisy, in situ images of high-aspect-ratio crystals to monitor particle size distribution. Chemical Engineering Science 61, 5236–5248.

Lee, K., Matsoukas, T., 2000. Simultaneous coagulation and break-up using constant-*n* Monte Carlo. Powder Technology 110, 82–89.

Legoux, J.G., Arsenault, B., Leblanc, L., Bouyer, V., Moreau, C., 2002. Evaluation of four high velocity thermal spray guns using WC–10%Co–4%Cr cermets. Journal of Thermal Spray Technology 11, 86–94.

Lei, S.J., Shinnar, R., Katz, S., 1971. The stability and dynamic behavior of a continuous crystallizer with a fines trap. A.I.Ch.E. Journal 17, 1459–1470.

Li, M., Christofides, P.D., 2003. Modeling and analysis of HVOF thermal spray process accounting for powder size distribution. Chemical Engineering Science 58, 849–857.

Li, M., Christofides, P.D., 2004. Feedback control of HVOF thremal spray process accounting for powder size distribution. Journal of Thermal Spray Technology 13, 108–120.

Li, M., Christofides, P.D., 2005. Multi-scale modeling and analysis of HVOF thermal spray process. Chemical Engineering Science 60, 3649–3669.

Li, M., Christofides, P.D., 2006. Computational study of particle in-flight behavior in the HVOF thermal spray process. Chemical Engineering Science 61, 6540–6552.

Li, M., Shi, D., Christofides, P.D., 2004a. Diamond jet hybrid HVOF thermal spray: gas-phase and particle behavior modeling and feedback control design. Industrial & Engineering Chemistry Research 43, 3632–3652.

Li, M., Shi, D., Christofides, P.D., 2004b. Model-based estimation and control of particle velocity and melting in HVOF thermal spray. Chemical Engineering Science 59, 5647–5656.

Li, M., Shi, D., Christofides, P.D., 2005. Modeling and control of HVOF thermal spray processing of WC–Co coatings. Powder Technology 156, 177–194.

Lih, W.C., Yang, S.H., Su, C.Y., Huang, S.C., Hsu, I.C., Leu, M.S., 2000. Effects of process parameters on molten particle speed and surface temperature and the properties of HVOF CrC/NiCr coatings. Surface & Coatings Technology 133.

Lin, Y., Sontag, E.D., 1991. A universal formula for stabilization with bounded controls. Systems & Control Letters 16, 393–397.

Lin, Y.L., Lee, K., Matsoukas, T., 2002. Simultaneous coagulation and break-up using constant-*n* Monte Carlo. Solution of the population balance equation using constant-number Monte Carlo 57, 2241–2252.

Lugscheider, E., Herbst, C., Zhao, L., 1998. Parameter studies on high-velocity oxy-fuel spraying of MCrAlY coatings. Surface & Coatings Technology 108–109, 16–23.

Ma, D.L., Tafti, D.K., Braatz, R.D., 2002. Optimal control and simulation of multidimensional crystallization processes. Computers and Chemical Engineering 26, 1103–1116.

Mhaskar, P., Gani, A., McFall, C., Christofides, P.D., Davis, J.F., 2007. Fault-tolerant control of nonlinear process systems subject to sensor faults. A.I.Ch.E. Journal 53, 654–668.

Miller, S.M., Rawlings, J.B., 1994. Model identification and control strategies for batch cooling crystallizers. A.I.Ch.E. Journal 40, 1312–1327.

Ramkrishna, D., 1985. The status of population balances. Reviews in Chemical Engineering 3, 49–95.

Rawlings, J.B., Sink, C.W., Miller, S.M., 1992. Control of crystallization processes. In: Industrial Crystallization—Theory and Practice, Boston, Butterworths, 1992, pp. 179–207.

Rawlings, J.B., Miller, S.M., Witkowski, W.R., 1993. Model identification and control of solution crystallization process—a review. Industrial & Engineering Chemistry Research 32, 1275–1296.

Rohani, S., Bourne, J.R., 1990. Self-tuning control of crystal size distribution in a cooling batch crystallizer. Chemical Engineering Science 12, 3457–3466.

The International Technology Roadmap for Semiconductors, 2005. Semiconductor Industry Association. San Francisco, CA.

Semino, D., Ray, W.H., 1995a. Control of systems described by population balance equations—I. Controllability analysis. Chemical Engineering Science 50, 1805–1824.

Semino, D., Ray, W.H., 1995b. Control of systems described by population balance equations-II. Emulsion polymerization with constrained control action. Chemical Engineering Science 50, 1825–1839.

Shi, D., Li, M., Christofides, P.D., 2004. Diamond jet hybrid HVOF thermal spray: rule-based modeling of coating microstructure. Industrial & Engineering Chemistry Research 43, 3653–3665.

Shi, D., Mhaskar, P., El-Farra, N.H., Christofides, P.D., 2005. Predictive control of crystal size distribution in protein crystallization. Nanotechnology 16, S562–S574.

Shi, D., El-Farra, N.H., Li, M., Mhaskar, P., Christofides, P.D., 2006. Predictive control of particle size distribution in particulate processes. Chemical Engineering Science 61, 268–281.

Smith, T., Matsoukas, T., 1998. Constant-number Monte Carlo simulation of population balances. Chemical Engineering Science 53, 1777–1786.

Steinfeld, A., 2005. Solar thermochemical production of hydrogen—a review. Solar Energy 78, 603–615.

Swank, W.D., Fincke, J.R., Haggard, D.C., Irons, G., Bullock, R., 1994. HVOF particle flow field characteristics. In: Thermal Spray Industrial Applications, Proceedings of the 7th National Thermal Spray Conference, Boston, MA, 1994, pp. 319–324.

Vekilov, P.G., Rosenberger, F., 1996. Dependence of lysozyme growth kinetics on step sources and impurities. Journal of Crystal Growth 158, 540–551.

Wegner, K., Ly, H.C., Weiss, R.J., Pratsinis, S.E., Steinfeld, A., 2006. In situ formation and hydrolysis of Zn nanoparticles for H_2 production by the 2-step ZnO/Zn water-splitting thermochemical cycle. International Journal of Hydrogen Energy 31, 55–61.

Weiss, R., Ly, H., Wegner, K., Pratsinis, S., Steinfeld, A., 2005. H_2 production by Zn hydrolysis in a hot-wall aerosol reactor. A.I.Ch.E. Journal 51, 1966–1970.

Xie, W., Rohani, S., Phoenix, A., 2001. Dynamic modeling and operation of a seeded batch cooling crystallizer. Chemical Engineering Communications 187, 229–249.

Zhang, G.P., Rohani, S., 2003. On-line optimal control of a seeded batch cooling crystallizer. Chemical Engineering Science 58, 1887–1896.

Zhao, L., Maurer, M., Fischer, F., Lugscheider, E., 2004. Study of HVOF spraying of WC–CoCr using on-line particle monitoring. Surface & Coatings Technology 185, 160–165.